Suspension Polymerization of Vinyl Chloride. I. Influence of Viscosity of Suspension Medium on Resin Properties

A. F. CEBOLLADA, M. J. SCHMIDT, J. N. FARBER, N. J. CAPIATI, and E. M. VALLÉS, *Planta Piloto de Ingenieria Quimica, UNS–CONICET, (8000) Bahía Blanca, Argentina*

Synopsis

The suspension polymerization of vinyl chloride is studied in a bench-scale reactor adequately reproducing reaction conditions and resin properties of industrial relevance. The evolution of particle morphology is analyzed at different stages of conversion, and a model for particle formation is verified. The influence of viscosity of the suspension medium is analyzed in relation to molecular weight distribution and particle morphology.

INTRODUCTION

Approximately 80% of the total demand of poly(vinyl chloride) (PVC) is produced by the suspension process, while the rest corresponds to emulsion and mass polymerization.

The suspension PVC is characterized by its low cost and versatility of applications. The ability of the resin to incorporate different additives and plasticizers results in a wide spectrum of processing characteristics and final properties. The capacity and rate of absorption of modifiers is determined by the particle morphology, which is essentially dependent on the polymerization conditions. Flow properties and mechanical performance, both strong functions of the molecular weight distribution, are also largely established by the reaction conditions.

In order to properly control both morphological and molecular characteristics, it is necessary to understand the influence of different process variables, their sensitivity and interrelation.

The development of morphology in suspension PVC process has been treated in a number of contributions. Davidson and Witenhafer,[1] Barclay,[2] and Allsopp[3] presented mechanisms of particle formation.

Ueda et al.[4] conducted a photographic study of stirred and unstirred polymerizations in a bench-scale (10 L) reactor. However, the study was limited to low conversions (20%) and a water–monomer ratio of 10/1, conditions that do not prevail in industrial operation.

The only reported work performed in a large scale reactor (5000 L) has been presented by Johnson,[5] who studied the effects of agitation on morphology. Experimental data show considerable dispersion, and no details are reported on the polymerization conditions and characterization methods.

Journal of Applied Polymer Science, Vol. 37, 145–166 (1989)

CCC 0021-8995/89/010145-22$04.00

Lewis and Johnson[6] studied the effect of agitation on particle size distribution in different reactor capacities: bench, pilot plant, and industrial scales. No other important resin properties were analyzed.

Besides conventional suspension agents, secondary suspension agents or surfactants are added to modify surface activity in particular. Their effect has been studied by Benetta and Cinque,[7] who tried to correlate activity with chemical structure.

Cheng[8] and Cheng and Langsam[9] studied the suspension polymerization of vinyl chloride using hydroxypropyl methylcellulose (HPMC) as suspension agents, although some of the varieties used in their work are not currently available in the market. These authors analyzed the influence of molecular weight and chemical structure of the cellulose on the particle morphology.

In relation to characterization of PVC resins, the only systematic study has been presented by Lalet et al.[10]

An overview of previous contributions indicates that many important aspects are not yet well understood. This can be justified by the particular complexity of the heterogeneous multiphase reaction system, with phase ratios changing during the evolution of the reaction. Important scale-up problems have not been solved. Most modeling efforts are based on geometric similitude, but a complete geometric and dynamic similitude has not been approached.

Several reports are based on observations on a particular experimental condition, without clear understanding of the interrelation of the process variables. In other investigations, the experimental conditions are not applicable to industrial operation.

In the experiments we present herein, the particular choice of operation condition yields bounds for Weber number in agreement with those reported by Lewis and Johnson[6] for bench-scale operation. As shown by these authors, such conditions permit reproducing the same particle diameter as obtained in industrial scale.

The present work is part of a wider approach oriented to the formulation of a complete kinetic model for the process, capable of correlating a variety of operation conditions with the resulting final properties in the resin. This goal implies, as a first step, a clear understanding of the influence of different process variables on molecular and morphological properties. The role of viscosity of the suspension medium on particle morphology is analyzed in subsequent sections. Additional kinetic information is obtained from studies of the evolution of conversion and properties in time.

PROCESS DESCRIPTION

The suspension polymerization process consists of suspending vinyl chloride monomer (VCM) in water, to form small droplets (0.01–0.02 mm in diameter). A free radical initiator and eventually a transfer agent are dissolved in the monomer, which is in the liquid state at current operating pressures. Given the high incompatibility between monomer and water, the reaction takes place essentially within the droplets, each one playing the role of an individual "bulk" reactor.[10–12]

These suspension systems are thermodynamically unstable, and are maintained by means of agitation and the use of suspension agents.[13,14] The main function of suspension agents is to prevent the coalescence of monomer droplets and to control the dimension and structure of particles during the polymerization. Water-soluble polymers are typically used for this purpose, i.e., modified cellulose and poly(vinyl alcohol)s with different degree of hydrolysis.[13]

EXPERIMENTAL TECHNIQUES

Equipment

Experiments were developed in a Sussmeyer Labo-Ind 30-L stirred tank, adequately modified to allow 15 kg/cm^2 maximum pressure (Fig. 1). The stirrer consists of a central propeller with three blades inclined 45°, developing a maximum of 300 rpm. The tank is provided with four baffles of circular cross section, placed at 4 cm from the reactor wall. Additional pieces of equipment

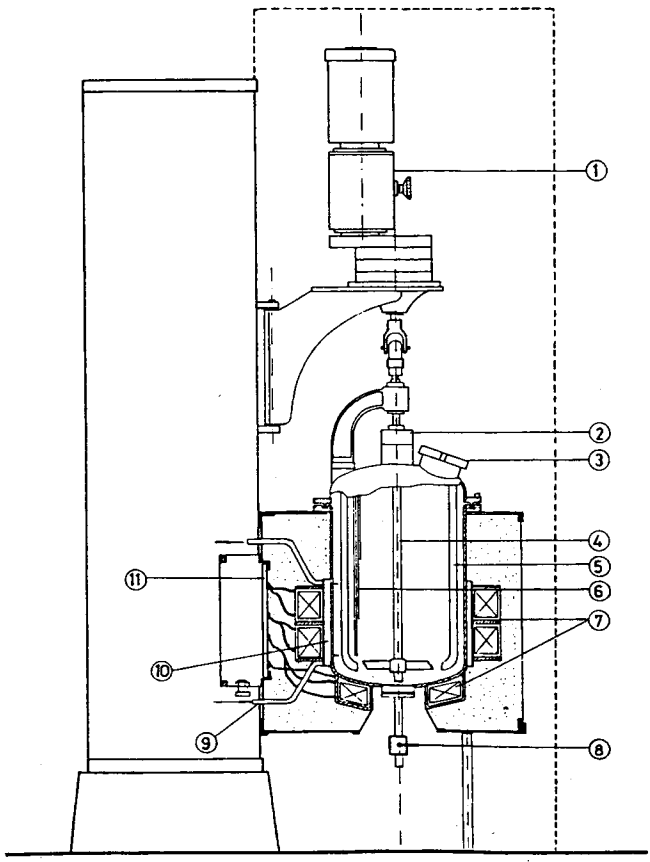

Fig. 1. Reactor schematic: (1) motor; (2) mechanical seal; (3) reactor vessel; (4) stirrer; (5) baffles; (6) thermocouple wells; (7) heating elements; (8) sampling device; (9) water inlet; (10) jacket; (11) electric board.

are required for loading and unloading, vacuum and pressurization, as well as safety devices due to the characteristics of VCM.[15-17]

A specially designed sampling device was constructed for measuring conversion vs. time and for tracking the morphological changes of the particles during the evolution of the reaction. The conversion vs. time relationship is obtained by weighing each sample, according to

$$C = \frac{M_p(1 + r)}{M_t} \tag{1}$$

where C denotes conversion, M_p is the mass of polymer in the sample, M_t is the total mass of sample, and r is the water–monomer mass ratio initially present in the reactor.[18]

The following reaction conditions were chosen, in agreement with industrial specifications:

Load temperature:	20 ± 1°C
Agitation speed:	230 rpm (corresponding to a tip speed of 1.8 m/s)
Initiator:	Lauroyl peroxide (0.26%, based on monomer weight), 10% solution in dichloroethane
Time for dispersion of initiator:	30 min
Mass of monomer:	10 kg
Mass of water:	17 kg
Suspension agent:	modified hydroxypropyl methylcellulose (HPMC), specified in each run (Table II)
Mixing time:	30 min
Heating time:	28 ± 1 min until reaching operation temperature
Reactor temperature:	60 ± 0.5°C
Initial pressure:	9.4 kg/cm^2
Final pressure:	3.5 kg/cm^2
Final conversion:	higher than 90%
Stripping of residual monomer:	1 h; 80°C, vacuum every 15 min
Sampling time:	30 or 60 min intervals, up to nine samples per run

Sampling

After a sample is obtained, the sampling device is submerged in liquid nitrogen to quench the reaction and to lower the vapor pressure of monomer. The sample is vented, after addition of ethanol to avoid foam formation and eventual mass loss. This procedure allows gradual pressure changes and slow vaporization of monomer within the particles, which is essential for protection of the fragile, low conversion structures. Samples are then washed, filtered, and dried.

Characterization of Suspension Media

Viscometry

Kinematic viscosities of suspension media were measured with a Cannon-Fenske 150 viscometer, calibrated at 60°C, according to ASTM norm 0445-53T.

Surface Tension

Surface tensions of suspension media were measured with a Du Noüy type tensiometer (Krüss K 8600), provided with a platinum ring of 1.91 cm diameter and 0.37 mm wire diameter (calibration at 60°C).

Molecular Properties of Resin

Gel Permeation Chromatography

Molecular weights were determined in a Waters ALC-GPC chromatograph equipped with refractive index detector and microprocessor, with four μ-Styragel columns of 500, 1,000, 10,000, and 100,000 Å mean pore diameter, respectively. The runs were performed at 25°C with a 1 mL/min flow rate using THF as the elution solvent.

The solvent was distilled in glass and refluxed for 2 h with 2% salicylic acid. The distillate was stabilized with 0.1% butyl hydroxytoluene (BHT), and filtered with 0.5 μm Millipore filters. Calibration was performed with seven polystyrene standards provided by Waters Associates, following Benoit's universal calibration method and using the following Mark–Houwink constants for PVC in THF at 25°C: $\alpha = 0.77$, $k = 1.5 \times 10^{-4}$ dL/g.

Morphological Properties

Porosity

Measurements were performed by mercury intrusion in a Super Pressure Inc. equipment, according to ASTM norm D 2873-70. From these data it was also possible to evaluate surface area following the technique proposed by Rootare and Prenzlow,[19] and mean pore diameter according to Washburn's equation.[20]

Granulometry

Particle size distribution and size averages were determined by two methods, fractionation according to ASTM norm D 1921-75, and particle counting in a Coulter Counter TA II equipment. A tube of 560 μm diameter was used for Coulter analysis. Samples of 20 mg of resin were contained in 250 mL of electrolite consisting of 1% solution of NaCl (in bidistilled water), and three drops of ethanol as dispersant. Calibration was performed with standard size particles of 42.54 μm diameter.

TABLE I
Characteristics of Hydroxypropyl Methylcellulose (HPMC) as Suspension Agent

HPMC types	Molecular weight range	Viscosity range[a]	Degree of substitution of *O*-methoxyl	Degree of substitution *O*-hydroxypropoxyl
F50	65,000–80,000	40–60	1.6–1.8	0.1–0.2
E50	65,000–80,000	40–60	1.65–1.9	0.2–0.3
E15	25,000–45,000	6–20	1.65–1.9	0.2–0.3

[a]2% weight solution, 20°C.

Electron Microscopy

Analysis was performed in a Jeol JSM-35 CF scanning electron microscope. Internal structure was studied by fracturing particles previously embedded in an acrylic resin.

Reagents

Vinyl chloride: industrial grade, from calcium carbide. Water: bidistilled, 0.5×10^{-6} Ω conductivity. Suspension agents: three varieties of modified cellulose (hydroxypropyl methylcellulose) (HPMC), METHOCEL E15LV, E50LV, and F50LV (Dow Chemical); specifications are summarized in Table I.[21] Initiator: lauroyl peroxide, technical grade.

RESULTS AND DISCUSSION

Conversion vs. Time

Conversion was calculated through the sampling procedure described in the previous section. Figure 2 contains the evolution of conversion and pressure in time, plotted simultaneously for four different runs. The trends are practically coincident, indicating the insensitivity of conversion to changes in properties of the suspension medium.

The reaction rate curve was obtained through numerical differentiation. The maximum reaction rate coincides with a sudden pressure drop in the reactor, attributed to the depletion of the liquid monomer phase.

Characterization of Suspension Media

The characterization of suspension media has been based on previous results by Cheng,[8] Cheng and Langsam,[9] and Sarkar.[21] From these conclusions and the features of the suspension agents employed (Table I), two main properties become evident in the characterization of suspension media: viscosity and surface tension in relation to the monomer (VCM). The former depends on the structure and molecular weight of the cellulose; the latter can be correlated with the surface tension of the continuous phase (water–HPMC) itself.

The dependence of viscosity and surface tension on concentration has been determined with the techniques already described. At 60°C and concentra-

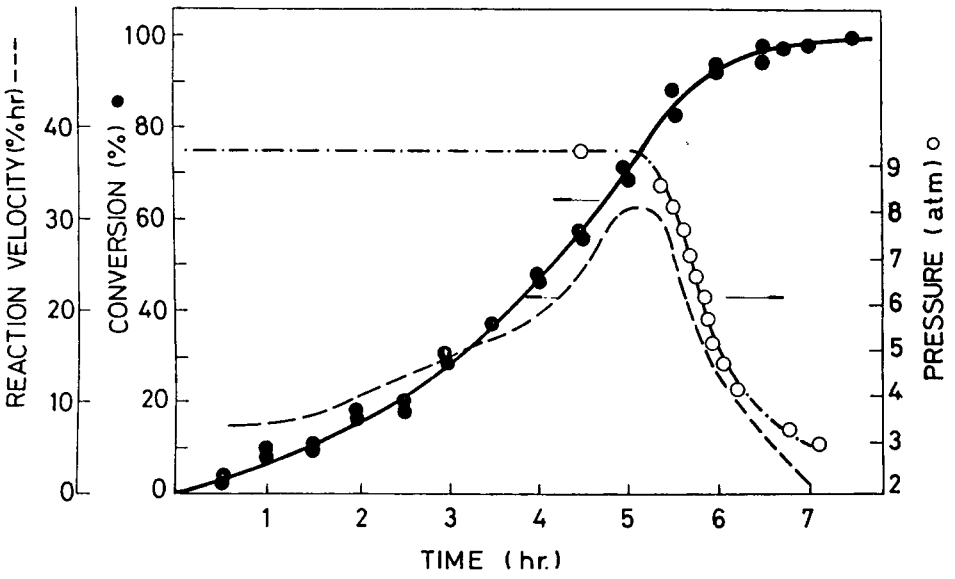

Fig. 2. Conversion, pressure, and reaction rate vs. time. Simultaneous plot for four different runs (60°C).

tions between 0.4 and 6 g/L, the following relations have been verified:

$$\log \nu = A + BC \tag{2}$$

$$\sigma = A' + B'C \tag{3}$$

where υ is the kinematic viscosity (cS), σ is the surface tension (dyn/cm), and C is the concentration of suspension agent (g/L water). A, B, A', and B' are constants determined for one suspension agent in particular, B, A', and $B' > 0$.

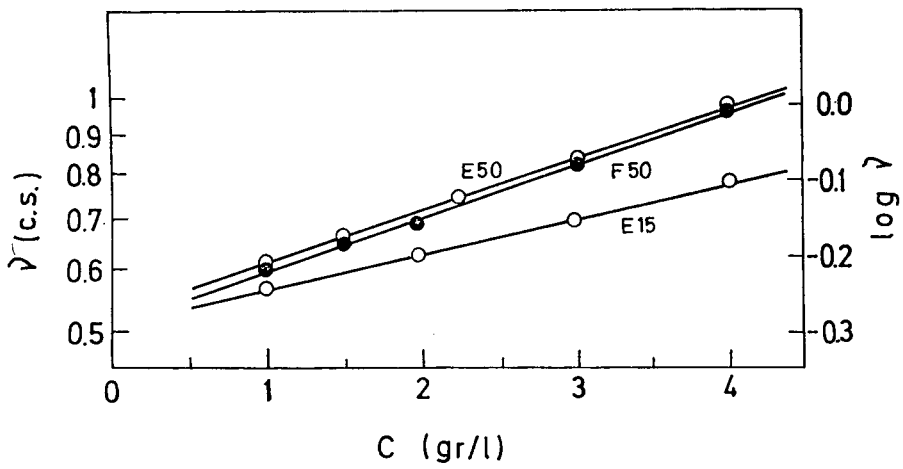

Fig. 3. Kinematic viscosity vs. concentration for three different HPMC suspension agents in water (60°C).

TABLE II
Characteristics of Suspension Media[a]

Run	Suspension agent	Concentration (g/L H_2O)	Viscosity[b] ν (cS)
1	E15	0.440	0.545
2	E15	0.644	0.556
3	E15	0.854	0.568
4	E15	1.343	0.593
5	E50	0.882	0.593
6	E15	3.000	0.708
7	F50	2.040	0.708
8	E50	2.990	0.820
9	E50	4.210	0.992

[a]Surface tension was almost constant in all runs ($\sigma = 45.4 \pm 2.7$ dyn/cm).
[b]At 60°C.

Experimental results for viscosity versus concentration are presented in Figure 3.

From the above relations, it was possible to program a series of suitable operation conditions allowing an independent analysis of the influence of viscosity at constant surface tension. Table II shows how the concentration and the suspension agent were changed in the different runs to obtain a significant variation of the characteristics of the suspension media.

Molecular Properties

The typical insensitivity of molecular weight averages during the evolution of conversion in free radical systems is also observed in this heterogeneous process. As predicted by a variety of models,[11,22] no significant changes are expected for the particular choice of initiator lifetime. This has been systematic for all runs. As an example, Table III shows the evolution of molecular weight averages with conversion for run 4. Figure 4 is based on the same experiments of Table III, and indicates no appreciable variations in the corresponding molecular weight distributions. The curves have been shifted vertically for comparison purposes.

The effect of properties of the suspension medium on molecular weight distribution has also been verified. GPC results for different runs, correspond-

TABLE III
Molecular Weight Averages vs. Conversion for Run 4

Conversion (%)	$\bar{M}_w \times 10^{-3}$	$\bar{M}_n \times 10^{-3}$	D (polydispersity)
6.0	72	42	1.71
11.3	75	44	1.70
18.1	75	41	1.83
35.3	72	44	1.64
60.3	73	41	1.78
91.3	79	44	1.80

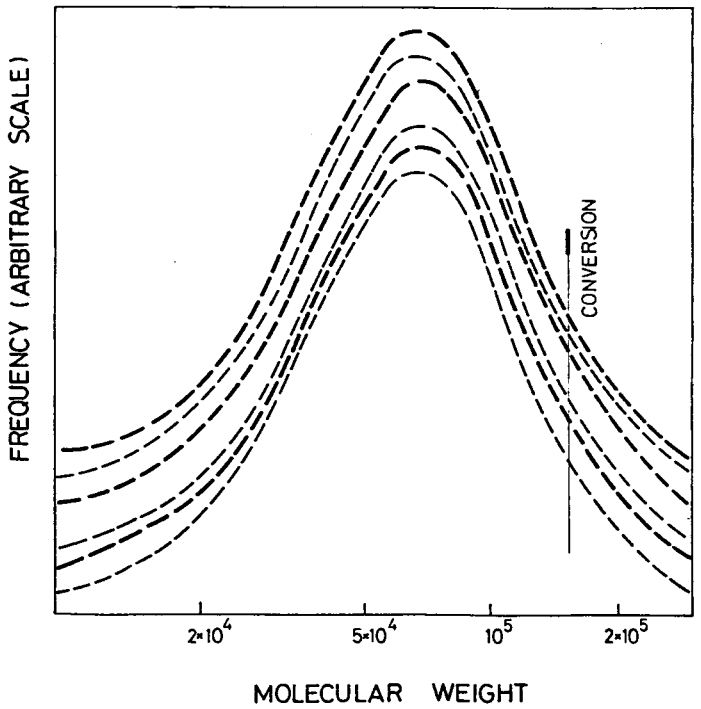

Fig. 4. Molecular weight distribution. Effect of conversion (run 4, 60°C).

ing to a variety of suspension agents and conversions higher than 90% in all cases, are summarized in Table IV and Figure 5. It can be concluded that there is no appreciable influence of the characteristics of the suspension medium on the molecular weight distribution.

Morphological Properties

The development of particle morphology during the evolution of conversion is analyzed for one suspension medium in particular. Later in this section, the effect of viscosity on physical structure is studied through comparison of high conversion resins related to a series of different suspension media.

TABLE IV
Influence of Properties of the Suspension Medium on Molecular Weight Averages

Run	$\bar{M}_n \times 10^{-3}$	$\bar{M}_w \times 10^{-3}$	$\bar{M}_z \times 10^{-3}$	$\bar{M}_v \times 10^{-3}$	$[\eta]$	D
1	47	83	185	77	0.90	1.77
4	44	79	170	75	0.88	1.80
5	48	88	205	81	0.94	1.83
6	45	83	181	77	0.90	1.84
7	43	79	169	73	0.86	1.84
8	46	81	204	80	0.93	1.76
9	49	91	236	83	0.96	1.86

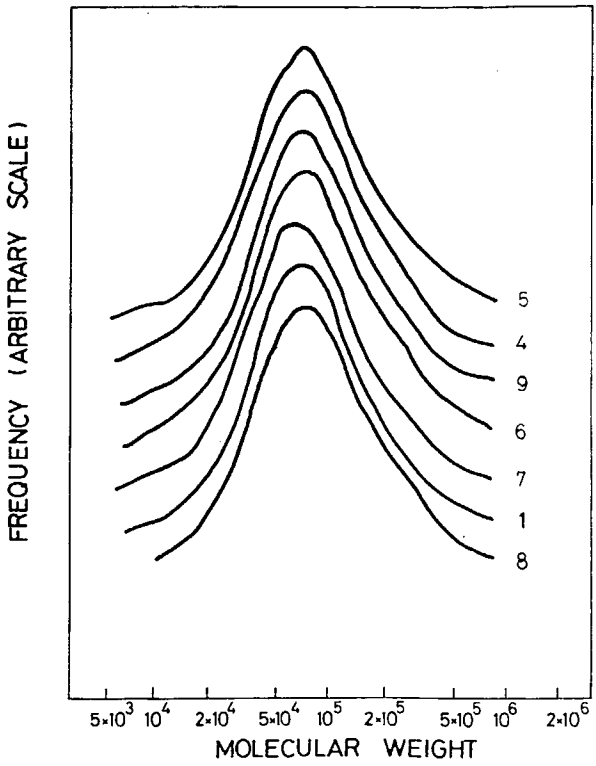

Fig. 5. Molecular weight distribution. Influence of properties of suspension medium for different runs at 60°C.

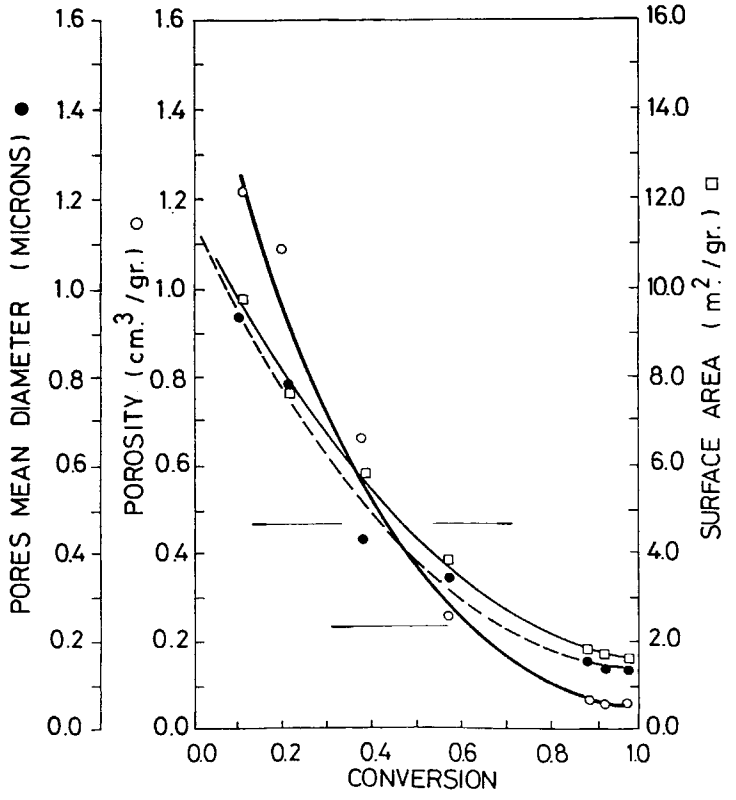

Fig. 6. Mean pore diameter (●), porosity (○), and surface area (□) vs. conversion (run 9, 60°C).

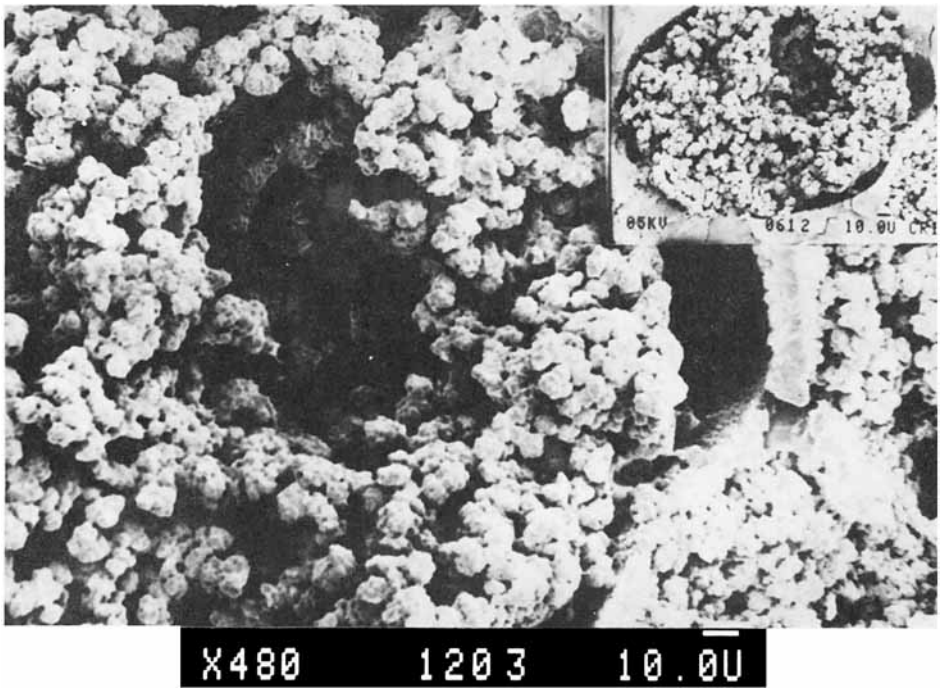

Fig. 7. PVC particle (× 480) (run 9, 18% conversion). Note the characteristics of the membrane surrounding the particle.

According to the proposed mechanism for particle formation,[1-3] it is expected that porosity, surface area, and mean pore diameter decrease with the progress of conversion. These trends are verified in Figure 6 for run 9. It is worth remarking that, at very low conversion, larger errors in porosity determinations are verified as a consequence of the fragile particle structures.

Two different stages of run 9 are also illustrated in Figures 7 and 8, corresponding to 18 and 93.9% conversions, respectively. Both micrographs, obtained at similar magnification (× 300) from fractured particles, clearly indicate the reduction of intraparticle volume with the extent of reaction. The formation of a membrane surrounding the particle is visualized in the detail of Figure 7.

The mechanisms of particle formation proposed by Allsopp[3] were also verified in detail. Figure 9 presents primary particles at very low conversions, 0.2–0.3 μm diameter (run 9, conversion below 1%). Figure 10 contains agglomerates of primary particles (run 9, 31% conversion). Figure 11 exhibits "fused primary particles" (run 9, 93.9% conversion).

The evolution of particle size with conversion is illustrated in Figure 12 (run 4, 11.3% conversion), and Figure 13 (run 4, 91.4% conversion).

Given the different nature of the methods, evaluation of diameters through Coulter Counter and fractionation (ASTM norm D 1921-75) did not yield totally coincident results. Nevertheless, the observed trends are the same in both cases.

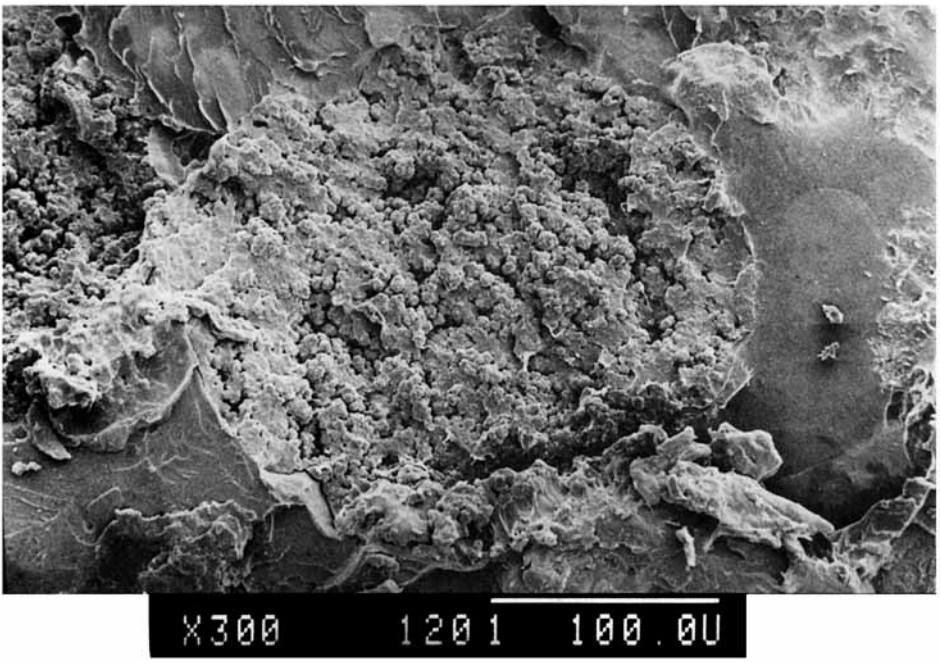

Fig. 8. PVC particle (× 300) (run 9, 93.9% conversion).

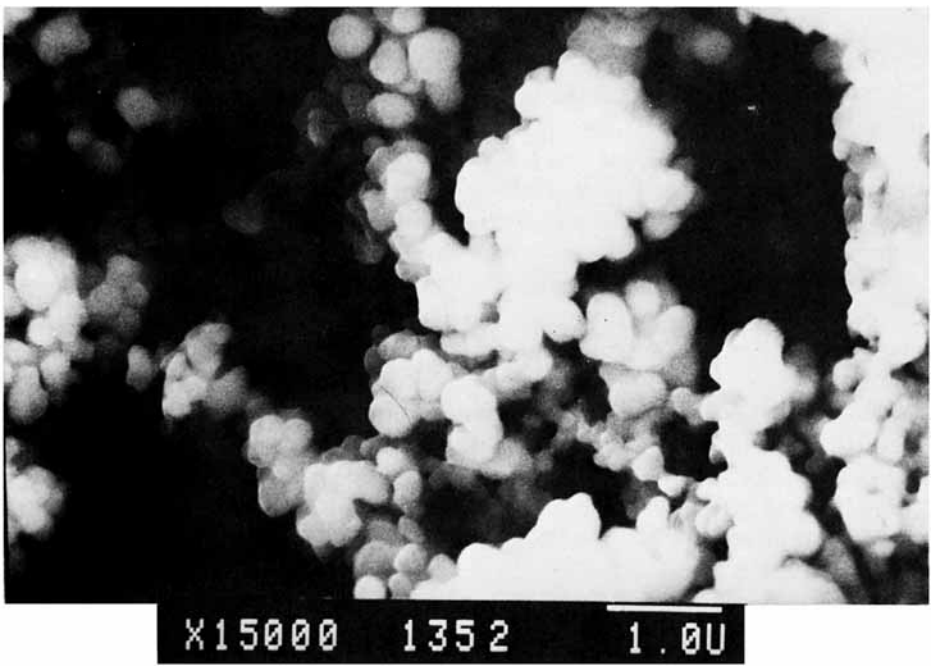

Fig. 9. PVC primary particles at very low conversion (× 15,000) (run 9, conversion below 1%).

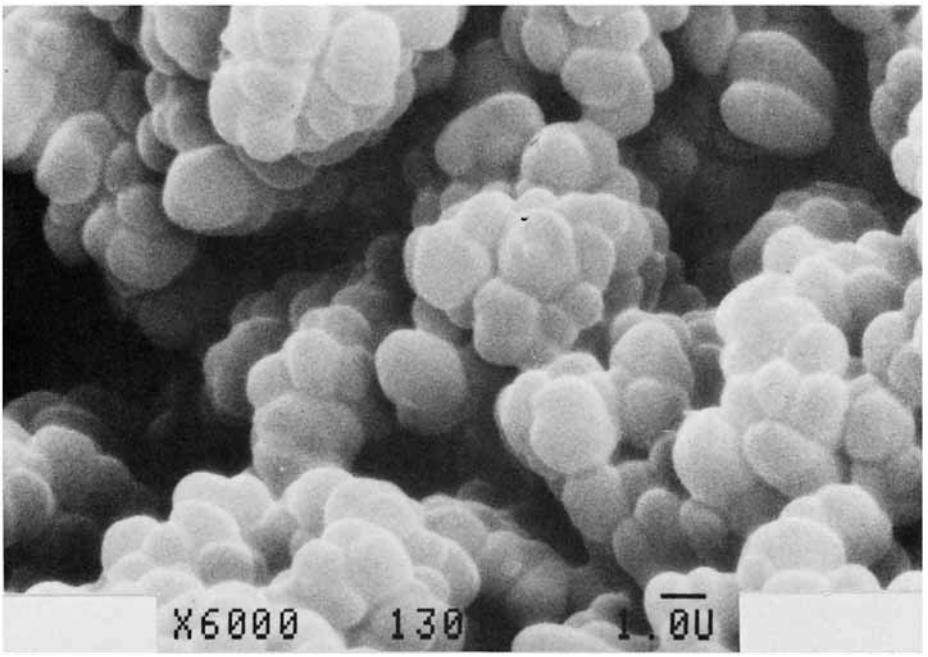

Fig. 10. Agglomerates of PVC primary particles (× 6000) (run 9, 31% conversion).

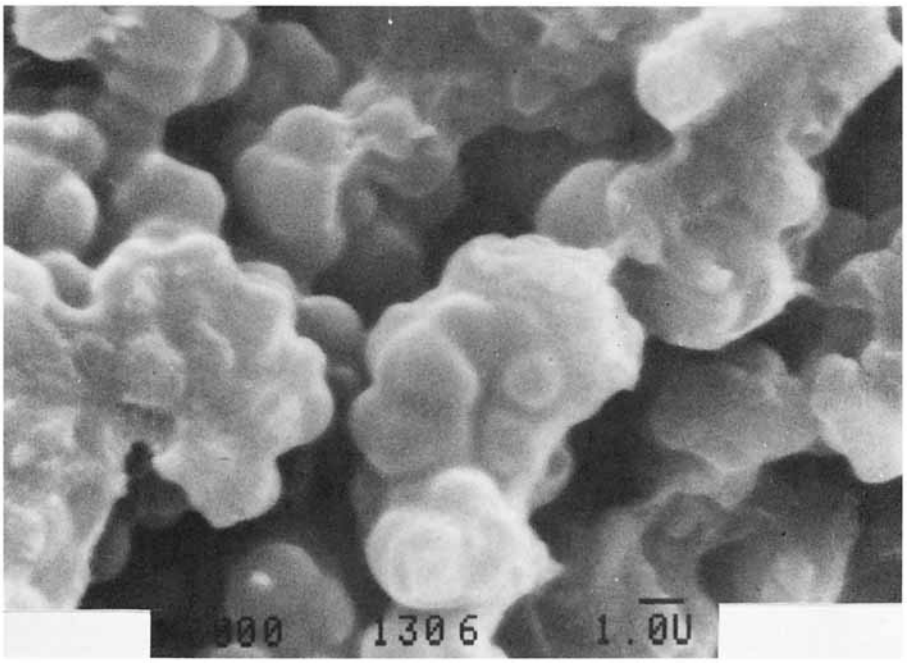

Fig. 11. "Fused" PVC primary particles (× 6000) (run 9, 93.9% conversion).

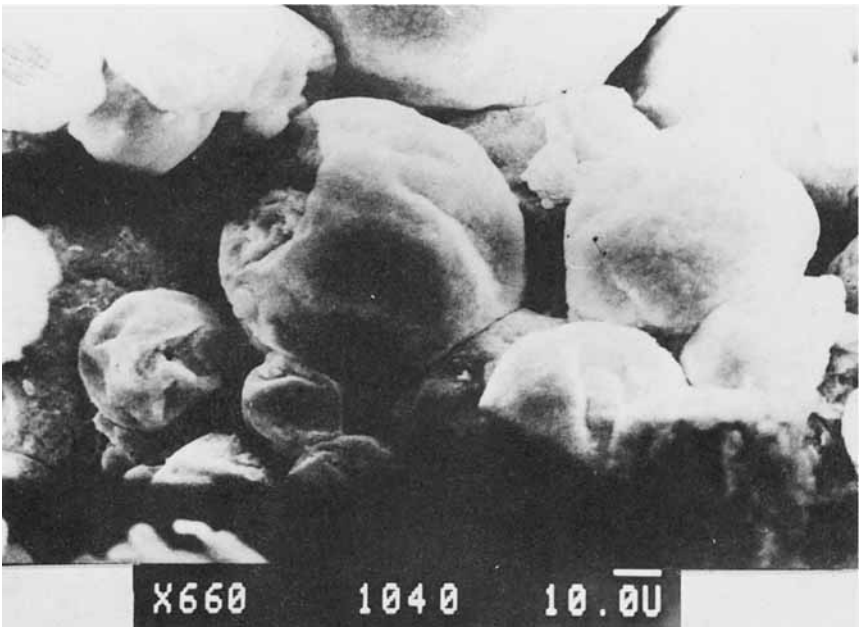

Fig. 12. PVC particle (× 660) (run 4, 11.3% conversion).

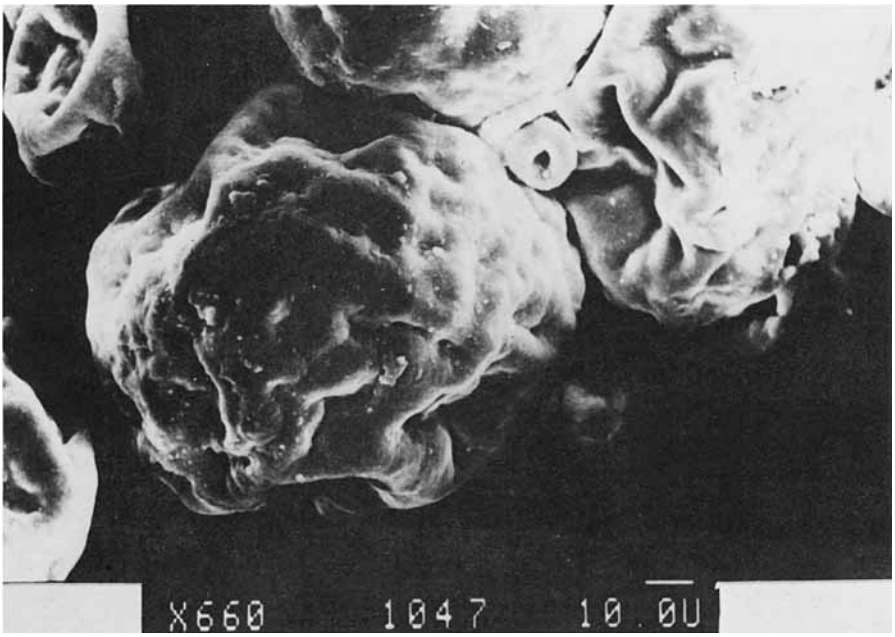

Fig. 13. PVC particle (× 660) (run 4, 91.4% conversion).

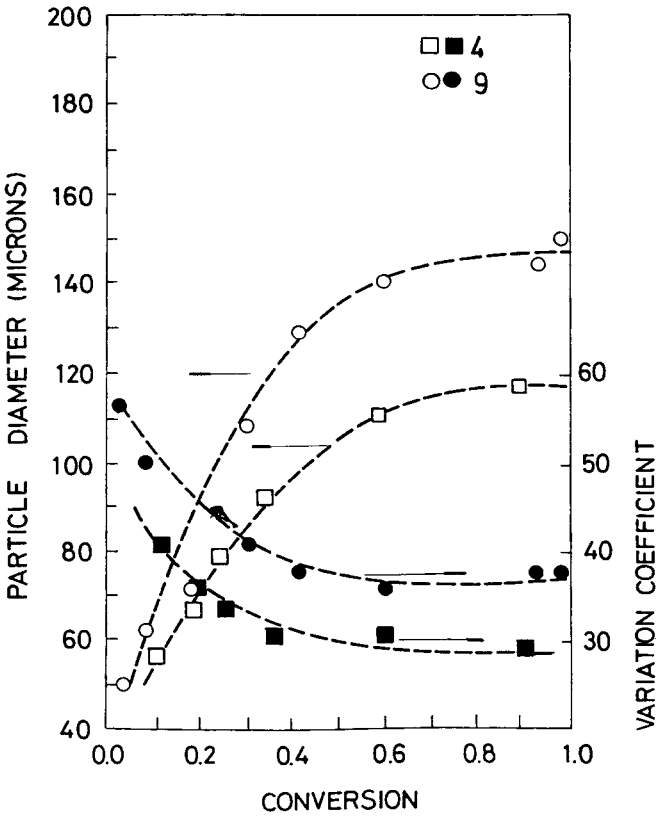

Fig. 14. Coulter Counter analysis. Mean particle diameter and coefficient of variation versus conversion [runs 4 (□,■) and 9 (○,●)].

The evolution of particle size with conversion was analyzed in a Coulter Counter equipment. Figure 14, based on runs 4 and 9, represents a typical granulometric analysis. Particle diameters exhibit a continuous increase until reaching conversions of about 70%. This trend has been verified systematically for all runs, as shown in Figure 15, where mean particle diameters are plotted relative to their final diameters at complete conversion.

The evolution of particle size distribution is analyzed through its coefficient of variation, VC (defined as the ratio between the standard deviation and the mean diameter) also reported in Figure 14. For all runs, it is observed as shown in the plot for runs 4 and 9 that the coefficient systematically stabilizes at a constant value at rather low conversions of about 35%. Runs 4 and 9 correspond to the extremes in the variation coefficient, run 4 being the one with narrower particle diameter distribution (VC = 30%) and run 9 the widest (VC = 38%). This behavior is consistent with the observation that the particle size distribution is essentially established in the early stages of the reaction. The rest of the section deals on the influence of viscosity of the suspension media on particle morphology.

In a liquid–liquid suspension, the maximum (critical) diameter allowing stable droplets without rupture or coalescence is known to increase with an

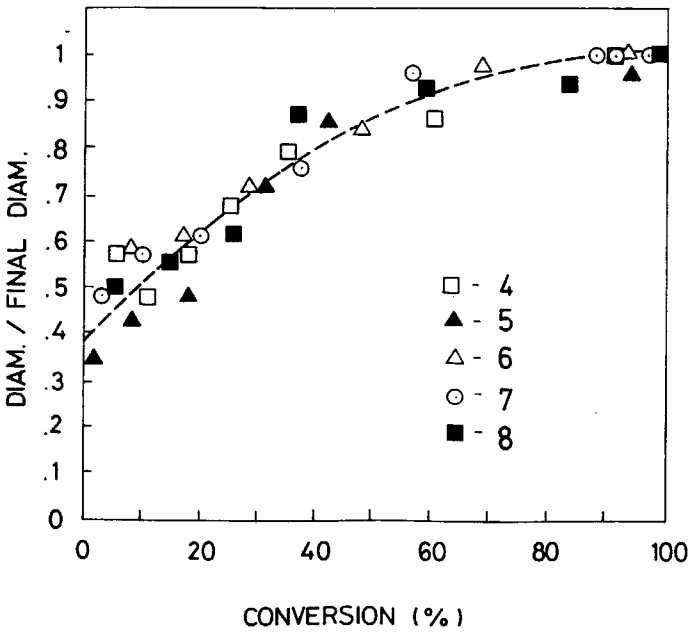

Fig. 15. Coulter Counter analysis. Relative mean particle diameter versus conversion (simultaneous plot for runs 4 (□), 5 (▲), 6 (△), 7(⊙) and 8(■)].

increase in viscosity in the continuous phase.[23] In the suspension system under study, an increase in viscosity results in a higher stabilization of the monomer droplets and the formation of unicellular particles or, equivalently, retaining their identity as droplets. Consequently, low viscosity media should produce smaller particles. This trend is verified in Figure 16, representing the variation of the final particle diameter with viscosity. For runs 6, 7, 8, and 9 a continuous decrease in particle diameter with decrease in viscosity of the suspension medium is observed. At the highest viscosity value, a considerable amount of rigid spherical particles is formed (see Fig. 17).

At lower viscosities, the mean particle diameter decreases continuously; however, coalescence mechanisms become active at a critical viscosity value leading to muticellular structures by agglomeration of particles. This is supported by particle size determinations (Table V) and micrograph analysis.

The effects of decreasing viscosity can be observed in the following micrographs, all of them corresponding to final conversion: Figure 17 (run 9, $\nu = 0.992$ cS) showing unicellular spherical particles of high diameter, Figure 18 (run 4, $\nu = 0.593$ cS) corresponding to an intermediate viscosity value, and Figure 19 (run 2, $\nu = 0.545$ cS) illustrating multicellular structures.

Figure 19 shows clearly that multicellular particles are composed of smaller particles of about 40 μm in diameter. If in Figure 16 a straight line is fitted through the experimental results from runs 6–9 where agglomeration mechanisms are not present, this is the diameter that corresponds to viscosities of the suspension medium of order $\nu = 0.556$ cS. At least from these results we may conclude that the diameter of individual particles decreases steadily with viscosity, but agglomeration leads to higher diameter particles.

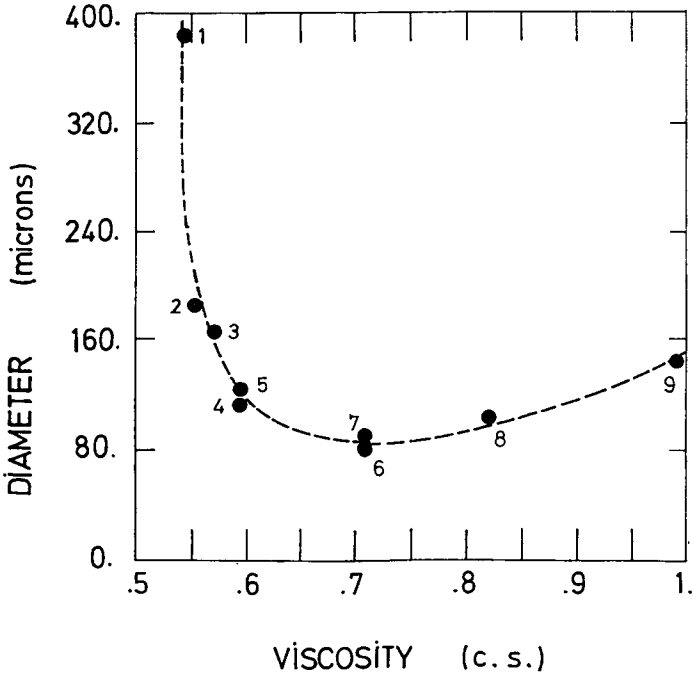

Fig. 16. Final particle diameter vs. viscosity (60°C).

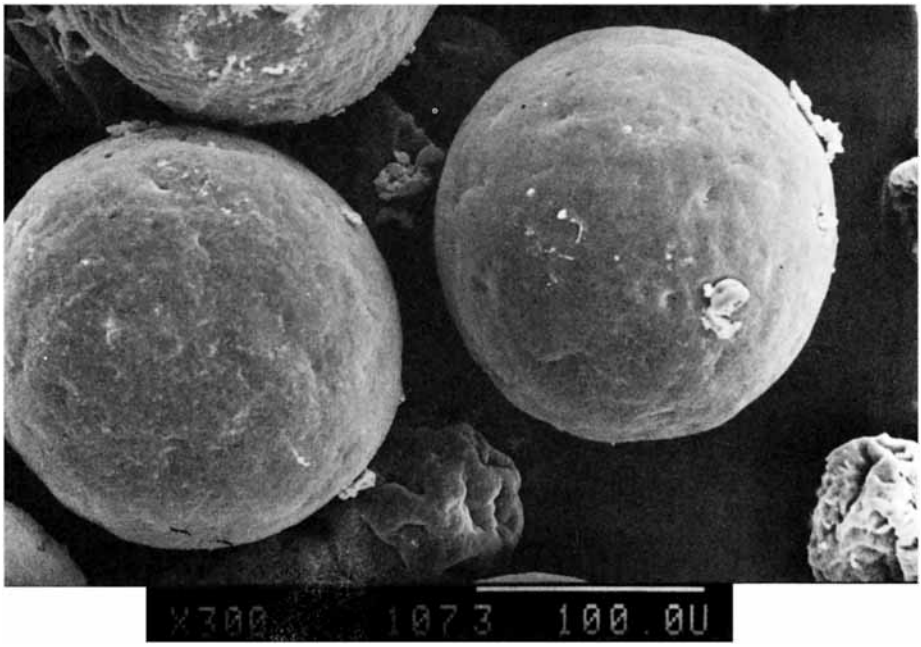

Fig. 17. PVC unicellular particles formed at high viscosity (× 300) (run 9, final conversion).

TABLE V
Influence of Properties of the Suspension Medium on Particle Size Distribution and Size Averages

Run	Porosity (cm^3/g)	Mean pore diameter (μm)	Mean particle diameter (μm)		Coefficient of variation (%) (Coulter)
			Coulter	Fractionation (ASTM)	
1	0.179	0.59	385	421	30.5
2	—	—	181	—	33.6
3	—	—	167	—	30.1
4	0.159	0.54	117	109	29.8
5	0.086	0.21	125	132	31.1
6	0.130	0.23	80	98	38.2
7	0.054	0.12	90	108	35.9
8	0.042	0.16	105	126	35.2
9	0.095	0.11	144	174	38.1

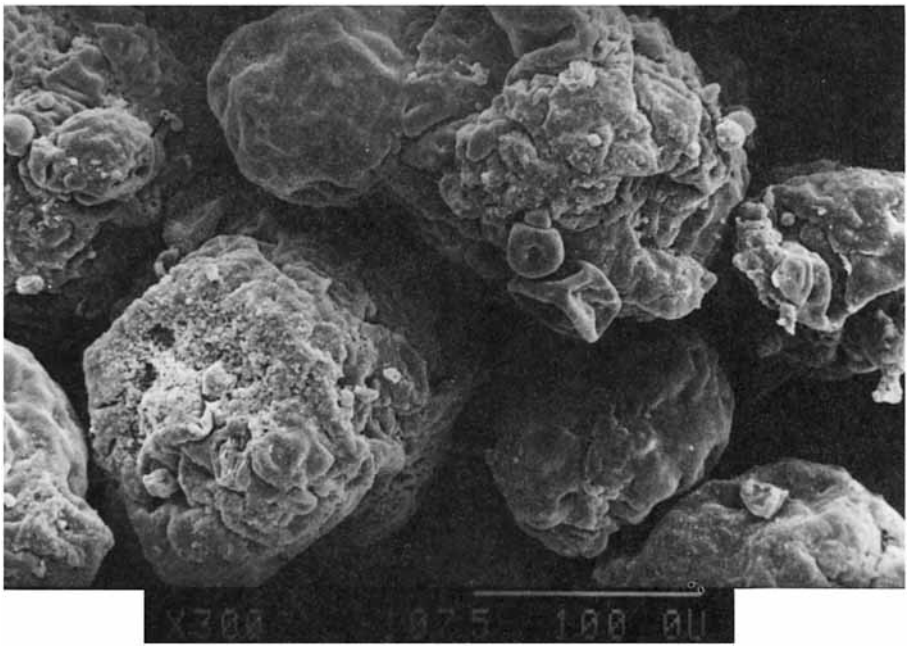

Fig. 18. PVC particle (× 300) (run 4, final conversion).

No significant influence of the molecular properties of the suspension agents on the external particle morphology was observed. In runs 4 and 5 two Methocel of different molecular weights were used in concentrations reproducing the same viscosity of the suspension media for both runs. The mean particle diameter was about the same in both runs; however, a considerable difference was observed in the internal morphology, as discussed below. The same kind of behavior was verified by comparing runs 6 and 7 in which two Methocel with different molecular weights and degrees of substitution were employed (see Tables II and V).

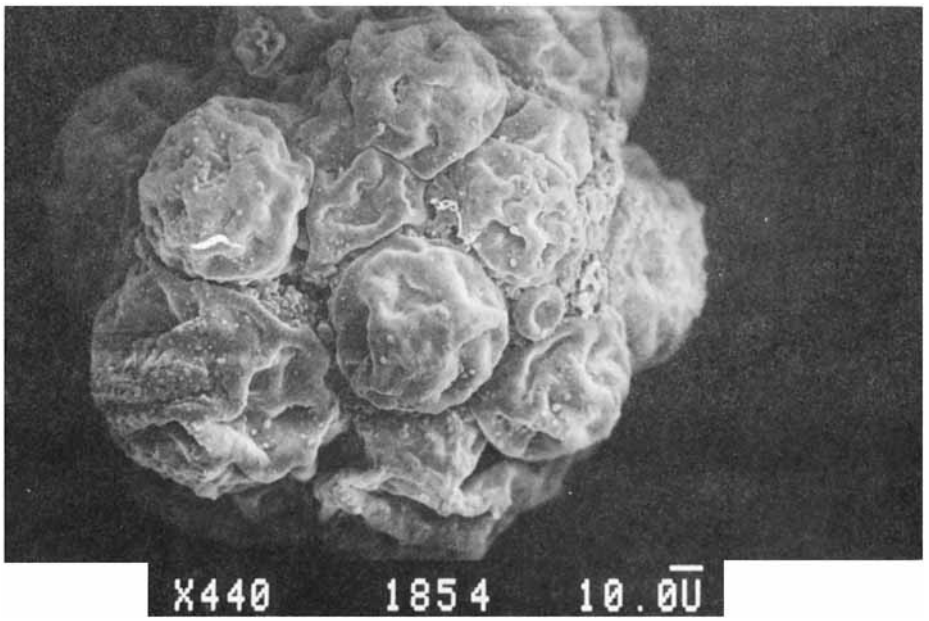

Fig. 19. PVC multicellular structures formed at lower viscosity (× 440) (run 2, final conversion).

According to these results, viscosity plays a fundamental role in the determination of particle size distribution. However, it bears no direct influence on the internal structure of particles. The internal porosity is instead controlled by the partition coefficient of HPMC between aqueous and monomer phase.[8,9] The HPMC–monomer compatibility is a function of the molecular weight and degree of substitution of the cellulose. Low molecular weights lead to higher compatibility and higher porosity in the final resin.

This trend can be verified by comparison of Figure 8 (run 9, high $\bar{M}_n$ of HPMC, $\nu = 0.992$) and Figure 21 (run 5, high $\bar{M}_n$ of HPMC, $\nu = 0.593$), with Figure 20 (run 4, low $\bar{M}_n$ of HPMC, $\nu = 0.593$), this last one exhibiting increased porosity. Similar trends are verified in Table V displaying porosity and mean pore diameter of particles at final conversion, for all runs.

Comparing results from two pairs of runs (6 and 7, 4 and 5), we observe that equal viscosities, obtained from appropriate concentrations of suspension agents of different molecular weights, result in similar final particle diameters at total conversion. The internal porosity depends instead on the molecular weight of the Methocel used in each case. Higher porosities correspond to lower molecular weights. It is also evident from Table 5 that, while intraparticle porosity dominates in high viscosity media, interparticle volume (among agglomerated particles) becomes relevant in the formation of the total porosity in low viscosity suspensions.

CONCLUSIONS

The suspension polymerizations of vinyl chloride has been studied in a bench-scale reactor, adequately reproducing reaction conditions and product specifications of industrial relevance.

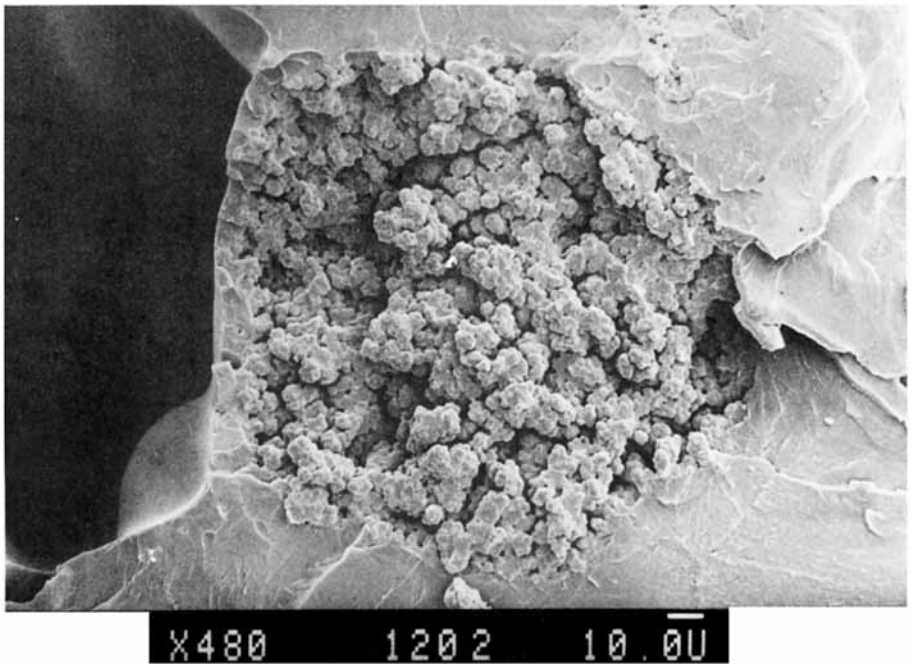

Fig. 20. Fractured PVC particle detailing internal structure (× 480) (run 4, final conversion).

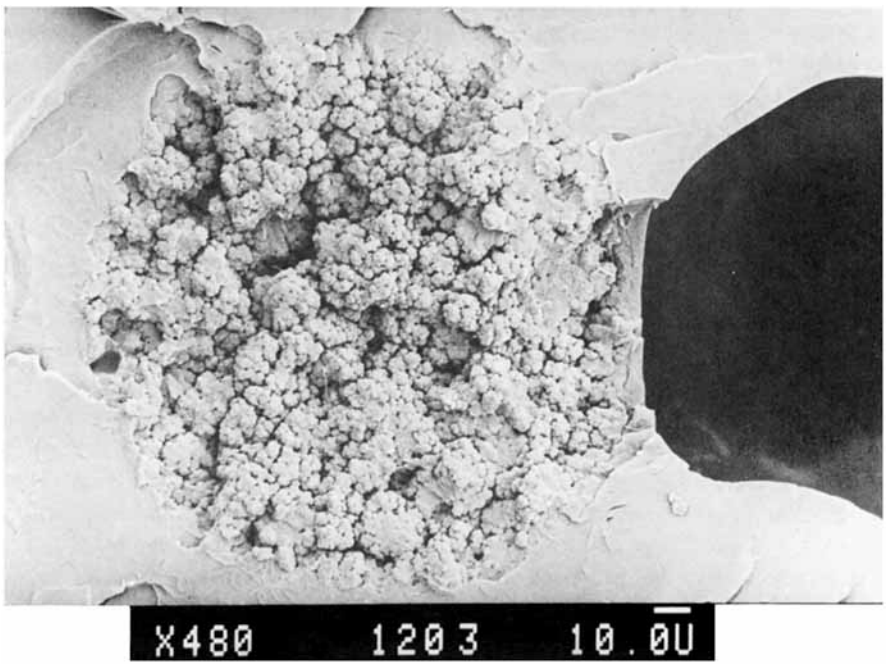

Fig. 21. Fractured PVC particle detailing internal structure (× 480) (run 5, final conversion).

A conveniently programmed set of reaction conditions allowed study of the evolution of conversion, particle morphology, and molecular properties in time. A previously proposed mechanism for particle formation has been verified. The set of experiments also allowed independent analysis of the influence of viscosity of the suspension medium on molecular weight and morphology.

Under concentration ranges typical for suspension polymerization, HPMC and other modified celluloses produce considerable increase in the viscosity of the suspension medium, and relatively minor changes in surface tension. The primary function of these suspension agents is stabilization through an increase in viscosity.

For a selected reaction condition, the molecular weight distribution and molecular weight averages remain practically unchanged during the evolution of the process. This characteristic of free radical systems is enhanced here by the particular choice of the initiator lifetime.

Under the selected experimental conditions, the molecular weights also remain insensitive to changes in viscosity of the suspension medium. For all practical purposes, viscosity bears no influence on the reaction kinetics. This "decoupling" of physical effects considerably simplifies on-going work oriented to the formulation of a complete kinetic model for the process.

In all samples, analysis of the evolution of particle morphology with conversion systematically indicates a decrease in internal porosity, which tends to level off at about 70% conversion. The mean particle size increases in a continuous trend and stabilizes after 60% conversion.

The situation is different in the case of particle size. As a consequence of the stabilizing effect, high viscosity media produce larger size, unicellular spherical particles retaining their identity as individual droplets. Conversely, low viscosity media favor the formation of smaller particles. At lower viscosities, however, coalescence mechanisms become active simultaneously, resulting in multicellular structures. As a consequence, particle size will exhibit a minimum at a critical value of viscosity when all other parameters are kept constant.

These preliminary findings are part of a wider approach toward a better comprehension of morphology formation and formulation of a kinetic model for the process.

The authors wish to thank INDUPA S.A. for providing the reagents and A. Sanger for assembling the equipment. This work has been supported by grants from CONICET, SECYT, and CIC.

References

1. J. A. Davidson and D. E. Witenhafer, *J. Polym. Sci., Polym. Phys. Ed.*, **18**, 51 (1980).
2. L. M. Barclay, *Angew. Makromol. Chem.*, **52**, 1 (1976).
3. M. W. Allsopp, *Pure Appl. Chem.*, **53**, 449 (1981).
4. T. Ueda, *J. Polym. Sci., Polym. Chem. Ed.*, **10**, 2841 (1972).
5. G. Johnson, *J. Vinyl Technol.*, **2**, 138 (1980).
6. G. M. H. Lewis and G. Johnson, *J. Vinyl Technol.*, **3**, 102 (1981).
7. G. Benetta and G. Cinque, *Chim Ind. (Milan)*, **47**, 500 (1985).
8. J. T. Cheng, *J. Macromol. Sci. Phys.*, **B20**, 365 (1981).
9. J. T. Cheng and M. Langsam, *J. Macromol. Sci. Chem.*, **A21**, 395 (1984).

10. M. M. Ph. Lalet, G. Pontalier, and Z. Vymazalova, *Plast. Mod. Elastomers*, **22**, 128 (1970).
11. G. Talamini and E. Peggion, *Vinyl Polymerization*, Dekker, New York, 1967, Vol. 1, p. 331.
12. G. Butters, *Particle Nature of PVC*, Applied Science, London, 1982.
13. L. I. Nass, *Encyclopedia of PVC*, Dekker, New York, 1976.
14. S. M. Ahmed, *J. Dispersion Sci. Technol.*, **5**, 421 (1984).
15. S. R. Sandler and W. Karo, *Polymer Synthesis*, Academic, 1977, Vol. II, p. 306.
16. J. C. Thomas, *J. Macromol. Sci. Chem.*, **A11**, 1553 (1977).
17. W. A. Mack, *Chem. Eng. Prog.*, **71**, 41 (1975).
18. A. F. Cebollada, unpublished results.
19. H. M. Rootare and C. F. Prenzlow, *J. Phys. Chem.*, **71**, 2733 (1967).
20. E. W. Washburn, *Proc. Natl. Acad. Sci. USA*, **71**, 273 (1967).
21. N. Sarkar, *J. Appl. Polym. Sci.*, **24**, 1073 (1979).
22. M. Ravey (Rogozinski), J. A. Waterman, L. M. Shorr, and M. Kramer, *J. Polym. Sci., Polym. Chem. Ed.*, **12**, 2821 (1974).
23. J. M. Church and R. Shinnar, *Ind. Eng. Chem.*, **53**, 479 (1961).

Received December 9, 1987
Accepted December 21, 1987